

MEASUREMENT AND ANALYSIS OF A 13 MEV CYCLOTRON MAGNETIC FIELD

S. H. Shin, M. Yoon, POSTECH, Pohang, Korea
E. S. Kim, K. H. Park, PAL, Pohang, Korea
J. S. Chai, KCCH, Seoul, Korea

Abstract

A four-sector 13-MeV cyclotron magnet, which does not employ the usual trim coils, was designed for positron-emission-tomography (PET) diagnostics. Instead, isochronism was achieved by placing a few side shims, as well as by slightly varying the vertical gap, along the radius of the cyclotron. The magnet was built based on the design, and its magnetic field was measured using a Hall probe. Equilibrium orbits were computed using the measured data. Then, a series of systematic optimizations of the magnetic field structure was performed. The final shape of the magnetic field was shown to satisfy the simultaneous requirements for isochronism and vertical focusing of the beam. Based on measured magnetic field, we designed a central region. The cyclotron has been routinely operationed at the Korea Cancer Center Hospital with a nominal beam current of around $50 \mu A$.

INTRODUCTION

PET cyclotrons are used to produce radio-isotopes such as ^{18}F whose lifetime is relatively short, about 110 minutes. At the Korea Cancer Center Hospital (KCCH) in Seoul, Korea, a project to build a 13-MeV PET cyclotron was carried out in a joint collaboration with Pohang University of Science and Technology (POSTECH).

In this paper, we introduce the major parameters of the 13-MeV PET cyclotron magnet with particular emphasis on the calculations of the equilibrium orbits from the measured magnetic field and beam dynamics in the central region. Table 1 shows the major design parameters for the 13-MeV PET cyclotron. A four-sector magnet structure was employed with a radial-ridged shape, and the minimal hill angle was chosen to be 30 degrees. For the ion source, an internal penning ion gauge (PIG) source was adopted. Based on the design, we built the magnet system in 2003 and performed a series of magnetic field measurements by using a Hall probe. During the field measurement, the field was progressively improved by successive mapping and shimming cycles. This paper is organized as follows: First, we describe the magnet and the field-measurement system. Analysis of the equilibrium orbit is then introduced, including isochronism, radial and vertical focusing, etc. The investigation of the central region is then described. Finally, a summary and conclusive remarks are given.

Table 1: Specifications for the magnetic field measurement system.

| Parameter | Unit | Value |
|-----------------|------|-------------------|
| Maximum energy | MeV | 13 |
| Beam species | | Negative hydrogen |
| Harmonic number | | 4 |
| Magnet Power | kW | 10.22 |

MAGNETIC FIELD

Based on the model, we fabricated the magnet and used a Hall probe to measure the resulting magnetic field. Figure 1 shows a block diagram of the field measurement system.

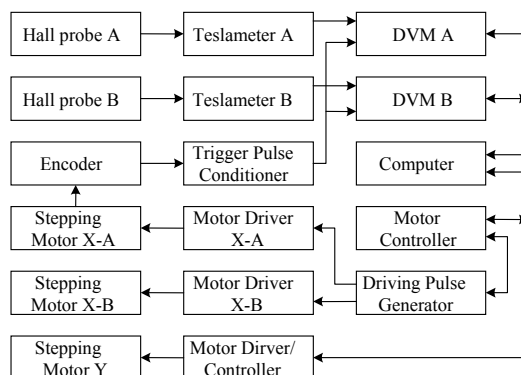


Figure 1: Block diagram of the field measurement system

The Hall probe is aligned within $50 \mu m$ and the resolution of the field measurement is 1 G. More details of the magnetic-field measurement system using a Hall probe is described elsewhere [1].

If the stability of particle motion in a given magnetic field is to be assured, equilibrium orbits must exist. Once an equilibrium orbit is found for a given energy, the revolution frequency along the equilibrium orbit is calculated, and the radial and the vertical transfer matrices are computed. These three parameters are then examined carefully to see if the field is isochronous with an acceptable phase excursion and with radial and vertical focusing without crossing harmful resonances. Figure 2 shows the average magnetic field as a function of the average beam radius. In this figure, the average magnetic

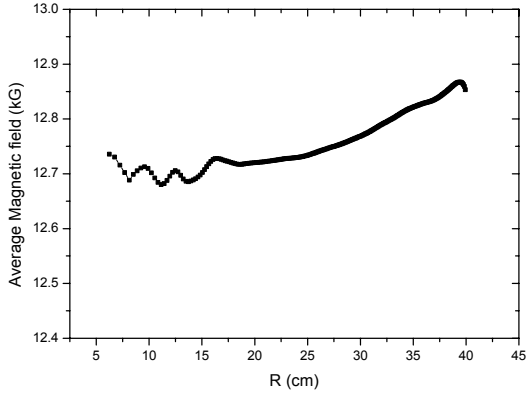


Figure 2: Average magnetic field along the average radius of the beam.

fields are the fields averaged along the equilibrium orbits. For the given magnetic fields, the equilibrium orbits are found by solving linearized equations of motion; the details can be found elsewhere [2]. Figure 3 shows the phase excursion as a function of the average radius of the beam, which was obtained from

$$\sin \theta(E) = \sin \theta_i + \frac{2\pi\hbar}{qV} \int_{E_i}^E \left(\frac{\omega_{rf}}{\omega(E)} - 1 \right) dE, \quad (1)$$

where ω_{rf} is a fixed frequency which is basically the radio frequency [3], $\omega(E)$ is the angular revolution frequency of a particle, qV is the peak energy gain per turn, and the integral extends from the initial energy E_i where $\theta = \theta_i$ to the given energy E . Figure 3 indicates that the total phase excursion is within ± 15 degrees.

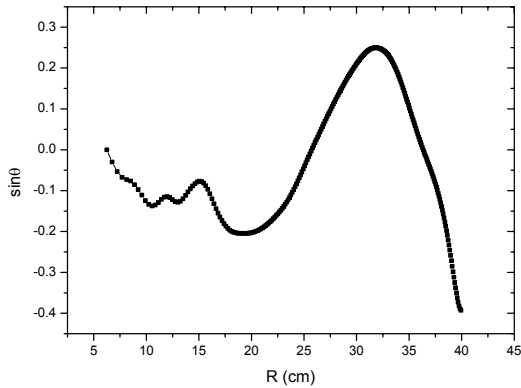


Figure 3: Phase excursion as a function of the average radius of the beam.

Other important parameters in beam optics are the radial and the vertical focusing frequencies, which are defined as the number of betatron oscillations per one revolution of a reference particle. These frequencies measure the degree of focusing in the radial and the vertical planes, respectively. Figures 4 and 5 show the computed radial and vertical focusing frequencies based

on the measured magnetic field. Figure 4 shows that between $R \sim 8$ cm and around 40 cm, ν_r is above the $\nu_r = 1$ resonance. However, around $R \sim 8$ cm, the beam passes through the $\nu_r = 1$ resonance. This is due to the small field bump applied near the center, as mentioned above. However, it is not so harmful to the beam because the beam passes through this resonance quickly due to the rather large turn separation. Near the extraction region, there is also a $\nu_r = 1$ resonance, but the beam is extracted before crossing this resonance.

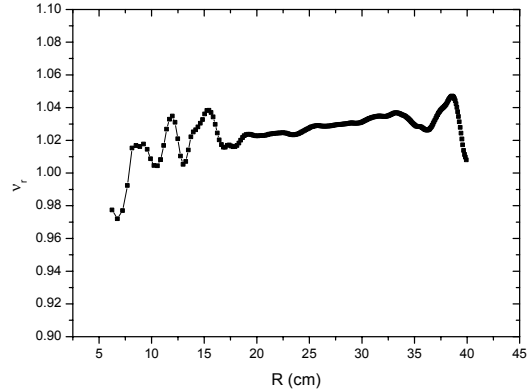


Figure 4: Radial focusing frequency as a function of the average radius of the beam.

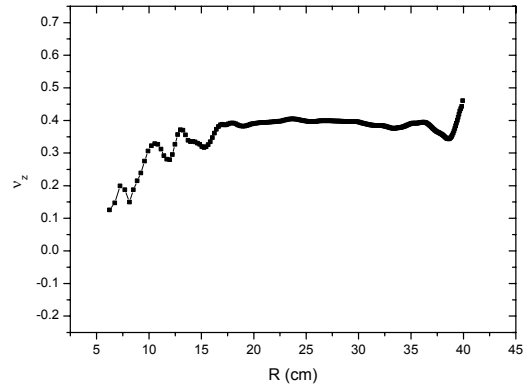


Figure 5: Vertical focusing frequency as a function of the average radius of the beam.

Figure 5 shows that ν_z is about 0.4, but particle crosses the $\nu_z = 1/3$ resonance near $R \sim 13$ cm. This resonance is driven by imperfect sextupolar fields and does not lead to beam loss.

CENTRAL REGION

Near the center of the cyclotron where magnetic field is too weak to provide a sufficient focusing and the field bump does not yet play a role in vertical focusing, an electric focusing is employed by means of dee tips. The central region in this paper means the region. To perform analysis of the ion trajectory in the central region, we first

assumed a specific geometry for the central region, considering the given initial energy gain. Subsequently, a three-dimensional distribution of the static electric field for this particular geometry was computed. The successive over-relaxation (SOR) method was adapted to calculate the three-dimensional electric potential in the quasi-static approximation [4]. We started with 4 mm meshes in order to cover the entire acceleration range of the cyclotron. The mesh size was then progressively reduced to 2 mm, 1 mm, 0.5 mm, and 0.25 mm. Then, scalar potentials in inner part of the relaxation volume were computed iteratively until they converged. The measured cyclotron magnetic field data was superimposed upon the rf field from the successive over-relaxation calculation. After tracing a particle for the first 20 turns, the radial motion, including orbit centering, was examined. The geometry was then improved accordingly, and the process was repeated. We obtained the centering of the reference particle by tracing the center of curvature of the particle at each point along the orbit, and the average center of these points was examined, trying to reduce it by repositioning the ion source and the puller. In a cyclotron, the vertical motion is very important because of the small gap. Figure 6 shows the vertical motion of two particles whose trajectories are orthogonal to each other. The starting conditions were $z = 0$ mm and $z' = 90^\circ$ for one particle and $z = 2$ mm and $z' = 0^\circ$ for the other particle. According to the linear theory, knowledge of the trajectories of these two orthogonal particles enables us to get trajectories of all other particles by linear superposition of these two particle trajectories.

CONCLUSION

So far, we have described the magnetic system and the central region of a 13-MeV cyclotron used for PET diagnostics. A four-sector magnet cyclotron without trim coils was designed with the help of the OPERA-3D program. Based on the design, we fabricated the magnet and measured its magnetic field by using a Hall probe.

The final shape of the cyclotron magnetic field was shown to satisfy the requirements for orbit stability, and vertical focusing. The electric-field distribution was obtained by solving Laplace's equation numerically. The central region was shown to have good centering and an adequately vertically focused beam.

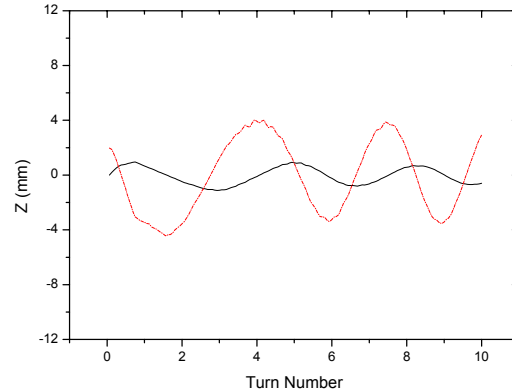


Figure 6: Vertical trajectories for two orthogonal particles.

REFERENCES

- [1] K. H. Park, Private communication.
- [2] H. L. Hagedoorn and N. F. Verster, Nucl. Instr. Meth. 18, 19, 201 (1962).
- [3] M. M. Gordon, Part. Acc. 16, 40 (1984).
- [4] M. Yoon and S. Oh, Nucl. Instr. Meth. Phys. Res. A 254, 477 (1987).